ACS Sustainable Resource Management

pubs.acs.org/acssrm

Article



# Closed-Loop Lithium Recovery from $LiFePO_4$ Batteries Using Tartaric Acid Leaching

Raffaele Emanuele Russo, Alessio Giampaoli, Martina Fattobene, Paolo Cognigni, Silvia Zamponi, Paolo Conti, Mario Berrettoni,* and Gabriele Giuli

Cite This: *ACS Sustainable Resour. Manage.* 2025, 2, 605−612

Read Online

ACCESS | Metrics & More | Article Recommendations | Supporting Information

**ABSTRACT:** This study investigates the sustainable recovery of lithium from spent $LiFePO_4$ batteries using tartaric acid derived from agro-food waste. To optimize both leaching and recovery processes, a fractional factorial design was first used to identify the key factors, followed by a central composite design for the process optimization. The optimal conditions, 2.1 M tartaric acid and a solid-liquid ratio of 110 g/L, achieved a lithium leaching efficiency of 95.0% (±2.3). The recovery of tartaric acid for reuse in multiple cycles was also optimized. Validation with real leaching solutions consistently demonstrated high recovery efficiencies with 98.0% (±1.9) of calcium tartrate and 97.7% (±3.6) of lithium phosphate. This study highlights the effectiveness of tartaric acid from agri-food waste for lithium leaching, promoting resource sustainability, and aligning with green chemistry principles. The findings provide a viable and efficient solution for industrial lithium recovery applications.

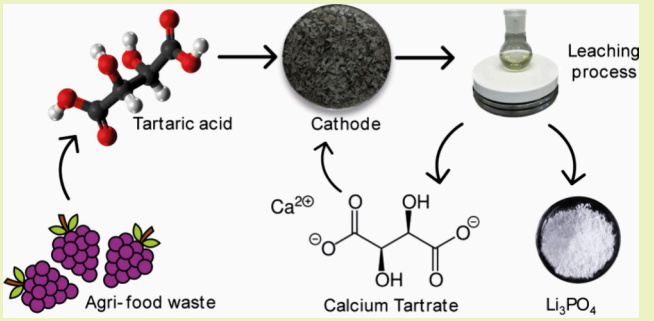


**KEYWORDS:** *Lithium iron phosphate, green process, tartaric acid, agri-food wastes, experimental design, metals recovery*



## INTRODUCTION

Lithium-ion batteries (LIBs) have become indispensable in modern technology due to their high energy density, long cycle life, and low self-discharge rates.[1] Since their commercial introduction by Sony in 1991,[2] LIBs have been widely adopted in portable electronic devices, electric vehicles, and renewable energy storage systems. Among the various types of LIBs, lithium iron phosphate ($LiFePO_4$) batteries are particularly noteworthy due to their high safety, thermal stability, and environmental friendliness.[3−5] However, the rapid increase in the consumption of $LiFePO_4$ batteries has led to an increasing volume of spent batteries, raising significant environmental concerns. For this reason, there is a need to develop efficient and sustainable recycling methods to recover valuable metals and mitigate environmental impacts. Lithium, as well iron, phosphorus, and vanadium, are a critical component of LIBs and essential for battery performance. The escalating demand for lithium, driven by the expanding EV market, underscores the need for effective recycling strategies to ensure a stable supply of this vital metal. Several studies have reviewed the latest techniques for recovering materials from spent lithium-ion batteries (LIBs).[6] Generally, the recycling process can be categorized into discharging and dismantling, pretreatment, metal leaching, and metal separation. Pretreatment methods, such as mechanical separation, ultrasonic cleaning, solvent dissolution, and ionic liquid dismantling, are crucial for isolating cathodic materials from the aluminum foil.[6] Hydrometallurgical methods have emerged as a promising approach for the recovery of metals from the spent LIBs. These methods involve the use of aqueous solutions to selectively leach metals from battery materials. Compared to pyrometallurgical processes, hydrometallurgical methods are more energy-efficient and generate less secondary pollution.[7] In recent years, researchers have increasingly used natural organic acids as leaching agents to mitigate adverse environmental impacts.[8] For example, citric acid has been used to achieve high recovery efficiencies for lithium, nickel, cobalt, and manganese from spent lithium nickel manganese cobalt oxide (NMC) batteries.[9] Similarly, oxalic acid has shown promising results in selectively recovering lithium and iron from spent $LiFePO_4$ batteries, with lithium leaching efficiencies reaching up to 98%.[2] Tartaric acid has also been effective in the recovery of lithium from spent LIBs.[10]

This research focuses on the use of tartaric acid, derived from agri-food waste, as a leaching agent for the recovery of lithium from spent $LiFePO_4$ batteries. Tartaric acid ($C_4H_6O_6$) is a naturally occurring organic acid commonly found in grapes

Received: December 4, 2024
Revised: March 13, 2025
Accepted: March 13, 2025
Published: March 24, 2025

and other fruits.[11] It is widely used in various industries, including food and beverage production, pharmaceuticals, and chemical manufacturing.[12] Its effectiveness as a leaching agent for metal extraction is due to its capability to form complexes with metal ions.[10] This study was inspired by one of the fundamental principles of chemistry, articulated by Antoine-Laurent Lavoisier: "Nothing is created, nothing is destroyed, everything is transformed".

Therefore, this research is dedicated to optimizing the lithium recovery process to maximize efficiency and sustainability. While the primary focus is on lithium extraction, the possibility of recovering the leaching agent is considered a subsequent step to further improve process circularity and minimize cost.

This comprehensive recovery strategy not only maximizes resource utilization but also adheres to green chemistry principles by minimizing waste production and reducing the demand for new reagents in each cycle. The influence of several process parameters on the leaching efficiency of lithium was systematically investigated. Additionally, the leaching kinetics were thoroughly analyzed. Following the leaching process, both tartaric acid and lithium were recovered. These comprehensive studies provide valuable insights into the efficient and sustainable recovery of lithium from spent batteries.

## METHODS

**Materials and Chemicals.** The discharged $LiFePO_4$ pouch cells used in this study were provided by Orim S.p.a., a company specializing in metal recovery from solid waste in Marche (Italy). We examined the cathodic active material extracted from these cells. Reagents and chemicals, including $HNO_3$ (65% pure), HCl (37% pure), and $H_2O_2$ (35%), were purchased from Sigma-Aldrich and used without further modification. NaOH, $CaCl_2$, and $Li_3PO_4$ were purchased by Sigma-Aldrich, while $Na_3PO_4$ was purchased by ThermoScientific. Tartaric acid ($C_4H_6O_6$) was obtained from Distillerie Mazzari S.p.a., an industry involved in recycling marc to recover the acid. Lithium, vanadium, iron, and, respectively, phosphorus standards were purchased from Carlo Erba and Sigma-Aldrich. Deionized water was employed in the leaching process and in the preparation of solutions for ICP-OES analysis.

**Analytical Methods.** Inductively coupled plasma optical emission spectrometry (ICP-OES) (model Thermo Scientific iCAP PRO X Duo) was used to measure the metal concentrations. Particle morphology and crystal structure were characterized by scanning electron microscopy (SEM-EDX) (model Zeiss Sigma 300) and X-ray diffraction (XRD) (model Philips PW 1830, Cu K$\alpha$, graphite monochromator), respectively. The calculated diffraction pattern was obtained using the Cambridge Crystallographic Data Center's (CCDC) mercury software. IR spectra were recorded with a PerkinElmer UATR two. Multivariate analysis was employed using the open-source software CAT (Chemometric Agile Tool).[13] All the analytical procedures are in the Supporting Information.

**Experimental Plan.** An experimental design approach was used to optimize the industrial hydrometallurgical process. A full factorial design with five factors varied at two levels would require at least $2^5 = 32$ analysis and would give information on the main effect of each factor and on all interactions between the different factors.[14,15] To limit sample analysis time and cost, a fractional factorial design $2^{(5-1)}$ with a resolution of V was performed. In total, 16 experiments were carried out in the fractional design matrix with the high and low levels represented by +1 and −1, respectively. Thus, a fractional factorial design was utilized to screen all the variables that can influence the system along with the respective range of variability. We examined five independent variables (factors) with the aim of distinguishing the significant ones from those with a negligible effect. The factors include the solid/liquid ratio (S/L) in g/L, the working temperature ($T$) expressed in degrees Celsius (°C), the reaction time ($t_r$) of the leaching process expressed in minutes (min), the concentration of tartaric acid ($[C_4H_6O_6]$) expressed in molarity (mol/L), and the concentration of hydrogen peroxide ($H_2O_2$) in volume %. According to the number of factors and their respective levels, the postulated multiple linear regression model (eq 1) is composed of 16 terms (1 constant, 5 linear terms, and 10 two-interaction terms) without confusion:

$$y = b_0 + b_1x_1 + b_2x_2 + b_3x_3 + b_4x_4 + b_5x_5 + b_{12}x_1x_2 + b_{13}x_1x_3 + b_{14}x_1x_4 + b_{15}x_1x_5 + b_{23}x_2x_3 + b_{24}x_2x_4 + b_{25}x_2x_5 + b_{34}x_3x_4 + b_{35}x_3x_5 + b_{45}x_4x_5 + \varepsilon \quad (1)$$

The factors were selected based on experience and classical leaching processes described in the literature.[10,16] Subsequently, a two-factor central composite, circumscribed design was developed to optimize the leaching process, with a total of 13 experiments with 5 replicates of the central point. It was chosen for only the significant variables. Thus, according to the number of factors and the respective levels, the postulated model is the full quadratic model composed of 6 terms (eq 2).

$$y = b_0 + b_1x_1 + b_2x_2 + b_{12}x_1x_2 + b_{11}x_1^2 + b_{22}x_2^2 + \varepsilon \quad (2)$$

Table S1 shows the variables together with their respective levels, both fractional design and central composite design.

For the recovery of tartaric acid, a full factorial design was used to study the effect of three variables: the stoichiometric ratio between lithium and precipitating agent (1:1 and 1:2, $x_1$), the physical state of the added salt (solid or liquid, $x_2$), and the washing process after filtration (with or without washing $x_3$). The percentage yield of calcium tartrate was determined using gravimetric analysis and used as a response. Concurrently, the purity of the precipitate was monitored to evaluate potential inclusions, occlusions, or coprecipitations of lithium at pH 7. This dual approach ensured a comprehensive assessment of both the yield and purity of the calcium tartrate precipitate. Table S2 shows the variables with their respective levels. Equation 3 shows the mathematical model with the main and interaction effects.

$$y = b_0 + b_1X_1 + b_2X_2 + b_3X_3 + b_{12}X_1X_2 + b_{13}X_1X_3 + b_{23}X_2X_3 + \varepsilon \quad (3)$$

The first variable was chosen to enhance the tartaric acid recovery efficiency. The other two categorical variables were selected for the same purpose and to mitigate the dilution effect caused by the addition of water, which reduces lithium concentration. Several studies indicate that high lithium recovery is achieved with concentrated solutions, so maintaining solution concentration was a key objective.[17] All of the experiments of each experimental design were conducted in a randomized order to eliminate any potential systematic biases that could affect the results. Instead, lithium precipitation has been widely investigated in the literature for its high efficiency.[17−20]

**Experimental Procedure.** The pouch cells were disassembled, and product analysis was conducted. The cathodic active material (containing lithium) was recovered through mechanical abrasion. This work was thoroughly characterized and used as the primary subject of the research. Aqua regia was used to dissolve it to measure the total amount of the metals (wt % total). Specifically, three tests were conducted with the heating plate set at 350 °C. Consequently, the total metal content was calculated as an average of these three trials. For the optimization of the leaching process, each experiment was carried out using the same leaching starting solution to maintain uniformity in measurement's errors. A condenser was used to prevent an increase in tartaric acid concentration when the temperature was set to high, while the stirring rate was kept constant at 300 rpm. Upon completion of the reaction, the solution was filtered and then filled to the desired volume in a volumetric flask. The metal content (wt % leaching) of the resulting leaching solution was then measured


https://doi.org/10.1021/acssusresmgt.4c00499
ACS Sustainable Resour. Manage. 2025, 2, 605−612

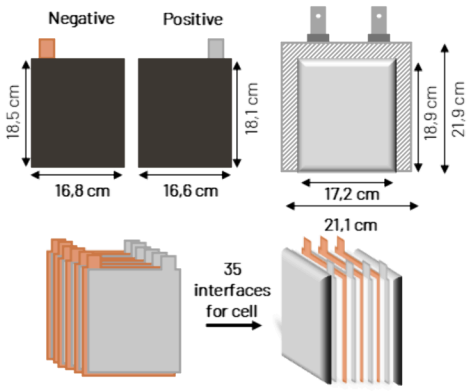


| Component | Average (g) | IC 95% |
|---|---|---|
| Pouch Cell | 774,88 | 4,18 |
| Without Casing | 732,93 | 4,20 |
| Casing, Tabs | 42,02 | 0,35 |
| Collector + | 12,26 | 0,18 |
| Collector-, Separator | 9,00 | 0,07 |

**Figure 1.** Product analysis of pouch cells.

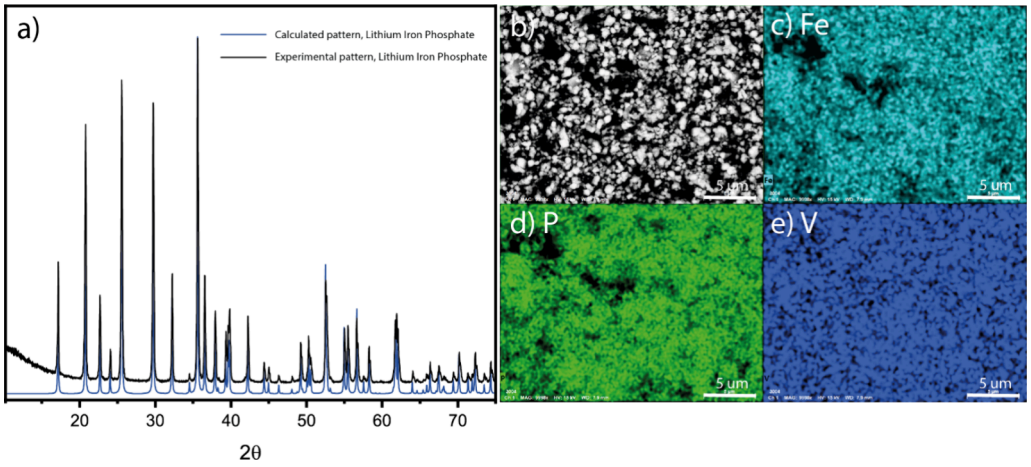


**Figure 2.** (a) XRD pattern of the active material of the cathode. (b) SEM image without EDX map, (c) iron EDX map, (d) phosphorus EDX map, and (e) vanadium EDX map. Magnification 9998× and bar = 5$\mu$m.

through ICP-OES, and leaching efficiency (LE) of each metal was calculated. For details, see the Supporting Information.

After the optimum experiment with the highest lithium leaching efficiency was determined, the precipitation processes for tartaric acid and lithium were examined in detail. The initial phase of the study involved synthetic solutions that mimic real-world conditions, followed by real leaching solutions derived from the cathode materials. To maintain the solution concentration and prevent excessive dilution, 10 M NaOH was used to adjust the pH to 7.0. At this pH, $CaCl_2$ was introduced as the precipitating agent. The resulting precipitate was filtered and dried for 24 h under low vacuum conditions. Subsequently, the pH of the solution was adjusted to 10.0 using additional NaOH, and $Na_3PO_4$ was added to precipitate $Li_3PO_4$. The precipitation experiment was conducted at 80 °C for 2 h with a stirring speed of 300 r/min and was repeated several times. Since the solubility of $Li_3PO_4$ decreases with increasing temperature, a higher temperature can make more Li precipitate. The precipitated $Li_3PO_4$ was then collected through filtration and washed with 80 °C deionized water to eliminate the excess $Na_3PO_4$. The Li contents before and after precipitation were measured by ICP-OES for the calculation of $Li_3PO_4$ precipitation (%).

## RESULTS AND DISCUSSION

**Disassembly and Characterizations.** Product analysis was conducted on five pouch cell batteries, providing both qualitative and quantitative information. This analysis allows for a comprehensive understanding of the waste material under investigation. In this context, the analysis is aimed at obtaining a detailed overview of waste and facilitating the planning of its recycling process. The operational procedure involves the separation of all of the components of each individual battery. At first, the pouch cells were weighed before manual disassembly. Each component was then weighed using an analytical balance, providing detailed measurements of each component's mass. This approach offers a comprehensive view of the sample being analyzed, allowing for a detailed assessment of the waste material. Figure 1 shows the product analysis.

The active material average of a cathode, calculated from three representative samples, was determined to be 10.51 g(±0.08). Given the total cathode mass of 12.26 g (Figure 1), it can be concluded that 86% of the cathode consists of active material.

The total metal content was determined through ICP-OES. It measured 5.54 ± 0.18 wt % of lithium, 19.91 ± 1.62 wt % of phosphorus, 32.37 ± 2.51 wt % of iron, and 0.25 ± 0.02 wt % of vanadium. The reported error is referred to only ICP analysis, based on three replicates. The XRD analysis, shown in Figure 2a, confirms the presence of a single crystalline phase in the sample. The calculated pattern of $LiFePO_4$ is represented by the blue line, while the experimental pattern is depicted by the black line. The comparison between the two lines demonstrates a close match, indicating $LiFePO_4$ as the only crystalline phase in agreement with literature.[21] SEM-EDX analysis (Figure 2b) shows that the sample consists of small, subspherical particles with a homogeneous particle size


https://doi.org/10.1021/acssusresmgt.4c00499
ACS Sustainable Resour. Manage. 2025, 2, 605−612

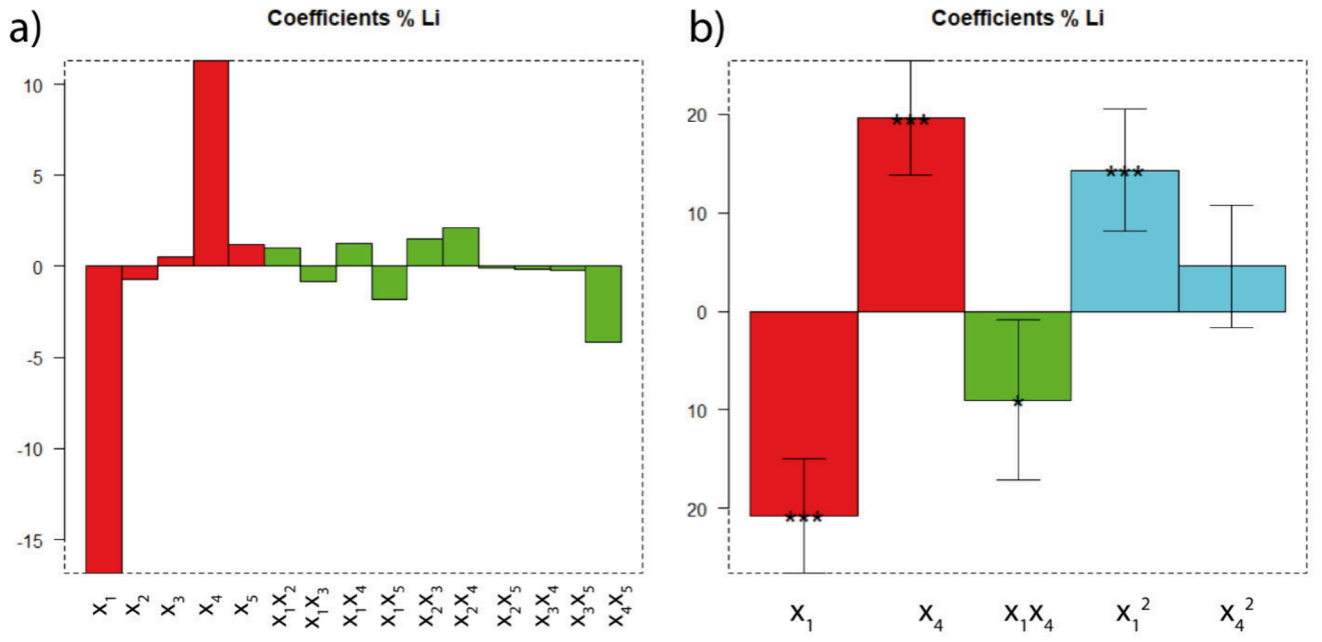


**Figure 3.** (a) Coefficient plot of fractional factorial design. (b) Coefficient plot of central composite design: the number of asterisks indicate the significance of coefficients, while the error bars indicate confidential interval error of the coefficients.

distribution ($\leq 5\mu$m). This information is important to study the kinetics of the process for applying the so-called model "Shrinking Core".[4,22,23] Furthermore, the metals exhibit a uniform distribution across the sample. Table S3 shows elemental analysis. The content of phosphorus, iron, and vanadium was compared with the ICP-OES analysis shown below (Figure 2c–e). Accounting for errors, both techniques indicate an identical percentage composition. Vanadium is used in batteries like a doping agent to improve performance.[24]

**Leaching and Recovery Mechanism.** Tartaric acid is a diprotic, dicarboxylic acid, and its dissociation reactions (eqs 4–5) can be represented as

$$H_2C_4H_4O_6 + H_2O \rightleftarrows H_3O^+ + HC_4H_4O_6^- \quad (4)$$

$$HC_4H_4O_6^- + H_2O \rightleftarrows H_3O^+ + C_4H_4O_6^{2-} \quad (5)$$

The $pK_a$ values of tartaric acid are $pK_{a1}$ = 2.72 and $pK_{a2}$ = 4.79 calculated by MarvinSketch developed by Chemaxon.[25] Theoretically, the leaching products can contain $Li^+$, $Fe^{3+}$, $PO_4^{3-}$, and vanadium. The leaching process can be described as a complexation and/or chelation phenomenon, where tartaric acid molecules envelop and bind to metals ions, forming stable complex compounds.[10,26−29] Computational studies have proposed complexes of tartaric acid with various metals, including lithium, for their potential use as leaching agents.[10] For the recovery of tartaric acid by precipitation, the salt with the lowest solubility constant ($K_{sp}$) was chosen to achieve a high-yield precipitate. Consequently, calcium tartrate was used by adding $CaCl_2$. The precipitation reaction was conducted at pH 7, where the molecular fraction $\alpha_{C_4H_4O_6^{2-}}$ is maximized, ensuring that almost 100% of the tartaric acid was the tartrate ion ($C_4H_4O_2^{6-}$). This approach ensures efficient precipitation and maximizes recovery. Equation S1 shows how the molecular fraction at pH 7 is calculated, and eq 6 shows the precipitation reaction.

$$C_4H_4O_6^{2-} + Ca^{2+} \rightleftarrows CaC_4H_4O_6 \downarrow \quad K_{ps} = 1.48 \times 10^{-7} \quad (6)$$

where $K_{ps}$ was calculated from the solubility of calcium tartrate, which is 0.1 g/L.[30]

For the recovery of lithium, a similar approach was utilized. An anion was chosen to form a salt with a low solubility product constant ($K_{ps}$). Specifically, $Na_3PO_4$ was selected as the precipitating agent to form $Li_3PO_4$, which has a low $K_{ps}$ of $2.37 \times 10^{-11}$ (eq 7).[31] The pH of the precipitation reaction was carefully selected based on the $pK_a$ values of phosphoric acid, $H_3PO_4$ ($pK_1$ 2.15, $pK_2$ 7.20, and $pK_3$ 12.15). These values indicate that a pH above 12 is necessary to maximize the concentration of $PO_4^{3-}$ ions, which is crucial for effective lithium precipitation. Additionally, $Na_3PO_4$, derived from a strong base and a weak acid, undergoes basic hydrolysis in solution (eqs 8–9), which increases the pH. Thus, the solution pH was adjusted to 10 using NaOH. Subsequently, $Na_3PO_4$ was added, exploiting its hydrolysis to further raise the pH without diluting the solution. As $OH^-$ ions form and the pH increases, the hydrolysis reaction is inhibited, thereby facilitating the precipitation of $Li_3PO_4$.[17] This method ensures that the solution remains concentrated, optimizing the lithium recovery process to gain a pH of about 10.

$$PO_4^{3-} + 3Li^+ \rightarrow Li_3PO_4 \quad (7)$$

$$Na_3PO_4 \rightarrow 3Na^+ + PO_4^{3-} \quad (8)$$

$$PO_4^{3-} + H_2O \rightleftarrows HPO_4^{2-} + OH^- \quad (9)$$

**Optimization of the Hydrometallurgical Process.** The leaching step was first addressed using a fractional factorial design (FFD) to identify the significant factors affecting the process. Following this, a circumscribed central composite design (CCC) was employed to optimize these factors. After conducting all the FFD experiments and collecting the results (expressed as a percentage of lithium leached) shown in Table S4, multiple linear regression (MLR) analysis was performed.


https://doi.org/10.1021/acssusresmgt.4c00499
ACS Sustainable Resour. Manage. 2025, 2, 605−612

Figure 3a illustrates the coefficient plot of the derived model, highlighting the impact of each factor on leaching efficiency. This approach ensured a systematic and thorough investigation, enabling the identification and optimization of critical parameters for the leaching process. As observed, the variables $x_1$ (solid-liquid ratio) and $x_4$ (tartaric acid concentration) play a significant role in the generated model. Specifically, an increase in the solid-liquid ratio correlates with a decrease in the leaching efficiency, as indicated by the negative coefficient. Conversely, an increase in the tartaric acid concentration correlates with an increase in leaching efficiency, as reflected by the positive coefficient. These findings highlight the importance of optimizing both the solid/liquid ratio and the tartaric acid concentration to enhance the overall efficiency of the leaching process.

Thus, a CCC design with only $x_1$ and $x_4$ was carried out. After running all the experiments and collecting the results (Table S5), a multiple linear regression (MLR) was carried out (eq 10). Stars represent the statistical significance ($p$-value; * = 0.05, ** = 0.01, *** = 0.001):

$$y = 18.3 - 20.7x_1(***) + 19.6x_4(***) - 9.0x_1x_4(*) + 14.3{x_1}^2(***) + 4.6{x_4}^2 \quad (10)$$

Figure 3b shows the coefficient plot for this model with the relative onfidence interval. The model has a SD of residuals of 6.9 (10 d.o.f.), an experimental SD of 4.0 (4 d.o.f.), an explained variance of 93.4, and an explained variance in prediction of 80.0. Since the residual standard deviation and the experimental standard deviation were not significantly different, there is no lack of fit. The linear terms for solid-liquid ratio ($x_1$) and tartaric acid molarity ($x_4$) variables are highly significant (both $x_1$ and $x_4$ at $p < 0.001$). Additionally, the interaction term for solid-liquid ratio and tartaric acid molarity ($x_1x_4$) is also significant ($p < 0.05$). The linear terms indicate that a more favorable response is achieved at lower solid-liquid ratios and higher tartaric acid molarities. Furthermore, the quadratic term of $x_1$ is also significant ($p < 0.001$). This suggests that lower solid-liquid ratios and higher tartaric acid concentrations result in improved leaching efficiency, likely due to the increased availability of the acid to interact with the solid material, thereby enhancing the leaching process. Figure 3a,b illustrates the previously discussed points. Figure S1 presents the response isosurface plot for the two variables considered. The optimal conditions for achieving high leaching efficiencies were identified in the upper left of the isosurface plot (black triangle in the Figure S1), with a tartaric acid concentration of 2.1 M and a solid-liquid ratio of approximately 100 g/L. Using the predictive model and despite the considerable error in this region, optimization aimed at maximizing the yield to 100% suggested an experimental point of 2.1 M tartaric acid and 110 g/L of active material. Three experiments conducted under these conditions showed a leaching efficiency of 95.0% (±2.3).

**Recovery of Tartaric Acid.** After the leaching optimization, the recovery process of tartaric acid was studied to enable its reuse in subsequent leaching cycles. Following this, the recovery of lithium was also examined. These dual approaches ensured that the process was both efficient and sustainable, maximizing resource utilization and minimizing waste. Before studying the precipitation process, a 2.1 M solution with added $CaCl_2$ was prepared. This experiment was useful to obtain a precipitate of calcium tartrate, which was used as a reference. An IR spectrum was conducted on this sample to confirm the correct precipitation of the calcium tartrate (Figure S2), followed by XRD analysis to identify the crystalline phase (Figure S3). The FTIR spectra obtained in this study are similar to the previously reported IR spectrum of calcium tartrate crystals.[32,33] The FTIR spectra confirm the presence of O−H, C═O, C−O, and Ca−O bonds in all samples, while the XRD pattern was confirmed by the ICDD database, which indicates a tetrahydrate calcium tartrate. This information was crucial, as it allowed us to calculate the right precipitation yield.

After performing all the experiments, a multiple linear regression analysis was conducted (eq 11). Table S6 presents the experiments and their corresponding experimental responses with an explained variance equal to 87.97%.

$$Y = 96.5 + 3.7X_1 + 0.3X_2 - 0.2X_3 + 0.6X_1X_2 + 0.6X_1X_3 + 0.7X_2X_3 \quad (11)$$

Figure S4 shows the coefficient plot. Notably, $x_1$ exhibits a larger magnitude compared to the other factors, indicating a stronger influence on the response variable $y$. This suggests that $x_1$ plays a critical role in driving the outcome. Specifically, it is reasonable to hypothesize that an increase in the stoichiometric ratio would positively affect the precipitation yield, which aligns with the underlying process dynamics. Thus, solid $CaCl_2$ was added in a stoichiometric ratio of 1:2 without washing, thereby preventing lithium dilution. Another experiment under these conditions was conducted to study repeatability, yielding a recovery rate of 99.8% (±2.8). An FTIR spectrum was acquired to confirm the successful precipitation and was subsequently compared to the reference spectrum for validation (Figure S2). All experiments consistently demonstrated a high purity of approximately 99.93% (±0.03) (Table S6).

Once the salt of tartaric acid is obtained, several efficient methods, already widely implemented on an industrial scale, can be used to produce tartaric acid. The conventional process involves crystallization in an acidic environment with $H_2SO_4$, which facilitates the removal of calcium ions by precipitating insoluble calcium sulfate ($K_{ps}$ of $9.1 \times 10^{-6}$).[34] Research has also increasingly focused on alternative, more cost-effective, and sustainable methods, such as electrodialysis and anion-exchange resins.[35−38]

**Recovery of Lithium.** An IR spectrum of the starting material $Li_3PO_4$ was recorded and used as reference (Figure S5). Thus, for subsequent trials (in synthetic and real solution), each precipitate was compared by performing IR spectroscopy and comparing the results with the standard IR spectra. In the pure $Li_3PO_4$ spectra, 1015 and 586 $cm^{-1}$ represent vibration of the $PO_4$ group.[39,40] Subsequently, lithium was precipitated as lithium phosphate in synthetic solutions. In this study, it achieved a recovery yield of 94.0% (±1.8). The error in these steps indicates the standard deviation calculated in two replicates. An FTIR spectrum was acquired to confirm the successful precipitation and was subsequently compared with the standard spectrum for validation (Figure S5).

**From Synthetic to Real System.** The developed precipitation process was then applied to the real leaching solution obtained by the leaching optimization procedure. Comparable recovery efficiencies were achieved, confirming the robustness and reproducibility of the process. 98.0% (±1.9) calcium tartrate and 97.7% (±3.6) lithium phosphate


https://doi.org/10.1021/acssusresmgt.4c00499
ACS Sustainable Resour. Manage. 2025, 2, 605−612

were recovered, respectively, with a purity of 99.5% and 99.9%. Figures S6–S7 present the FTIR spectra from the real-case test. Table 1 shows the mass balance calculated considering the

**Table 1. Mass Balance of the Process**[a]

| # | | Li | Fe | $H_2C_4H_1O_6$ | Ca |
|---|---|---|---|---|---|
| 1 | Starting solution | 6.05 | 35.64 | | |
| 2 | Leaching process ($m_i$) | 5.91 | 1.60 | 315.00 | |
| 3 | Adding $CaCl_2$ | | | | 126.25 |
| 4 | Calcium tartrate precipitation | 0.09 | 1.44 | 308.70 | 82.43 |
| 5 | Lithium phosphate precipitation | 5.68 | 0.00 | | 40.00 |
| 6 | $\Delta(m_i - m_f)$ | 0.14 | 0.16 | 6.30 | 3.82 |
| 7 | % | 2.38 | 9.88 | 2.00 | 3.03 |

[a]Row 1 is the total amount of metal in the starting material; row 2 is the initial mass for Li, Fe, and tartaric acid; rows 4 and 5 are the recovered steps for lithium and tartaric acid; rows 6 and 7 are the difference in mass between rows 2 and 4–5 in absolute and percentage, respectively. Residual calcium in row 5 is due to the stoichiometric ratio used for the tartaric precipitation.

optimized solid-to-liquid ratio of 110 g/L. Lithium, iron, calcium, and tartaric acids are reported. The mass balance is calculated by determining the difference ($\Delta$) between the initial mass ($m_i$) and final mass ($m_f$) in grams.

At this step, the recovered $Li_3PO_4$ could be reintegrated into industrial value chains. For instance, it is an essential component that serves as a raw material for lithium-ion batteries. Additionally, it is used in thin-film and glass-ceramic electrolytes, where it enhances ionic conductivity and stability.[41]

**Kinetics and Determination of the Rate-Controlling.** To study the leaching kinetics, a test was conducted using optimized conditions for lithium recovery. The objective was to analyze the leaching rate within a specific timeframe. The shrinking core model (SCM), widely used for leaching kinetics, was applied here to describe consecutive steps in the leaching process: diffusion of the reagent through a liquid film around the particles, diffusion through a solid product layer, and the dissolution reaction at the unreacted core surface, leading to metal mobilization. Each step has corresponding kinetic equations (eqs 12–14) that describe the process rate, with the equation best fitting the experimental data considered the rate-controlling step.

Film diffusion control:

$$t \propto X \tag{12}$$

Product layer diffusion control:

$$t \propto 1 - 3(1 - X)^{2/3} + 2(1 - X) \tag{13}$$

Chemical reaction control:

$$t \propto 1 - (1 - X)^{1/3} \tag{14}$$

where $t$ is the reaction time and $X$ is the fraction of leached metal. The kinetic data obtained from the different mechanisms (eqs 15–17) are presented in Figure 4a, indicating a change in slope around 3 min, suggesting a shift in the leaching mechanism. Thus, the kinetic data was analyzed in two phases. During the initial 3 min, the kinetic plots from eqs 12–14 are displayed in Figure 4b, showing the chemical reaction and film diffusion control equations with the highest $R^2$ value, indicating their dominance. The rate constant up to 3 min was calculated as an average result, 0.14 $min^{-1}$. For the second phase, starting at 5 min, new equations derived by Aarabi-Karasgani et al. were used (eqs 15–17),[42] capturing the leaching process behavior beyond the initial 5 min:

$$t - t_1 \propto X \tag{15}$$

$$t - t_1 \propto 3[(1 - X_1)^{2/3} - (1 - X)^{2/3}] - 2(X - X_1) \tag{16}$$

$$t - t_1 = (1 - X_1)^{2/3} - (1 - X)^{2/3} \tag{17}$$

where $X$ is the fraction of leached metal in the second stage, $t_1$ is the time at which the second stage started, and $X_1$ is the fraction of leached material at time $t_1$. Figure 4c shows $R^2$ values for the liquid film, product layer diffusion, and chemical control, which are very close, suggesting a mixed control mechanism. The rate constant was thus calculated as an average of each mechanism, resulting in a value of 0.009 $min^{-1}$.

## CONCLUSIONS

This study successfully demonstrated the sustainable recovery of lithium from $LiFePO_4$ batteries using tartaric acid derived from agro-food waste, in line with green chemistry principles by promoting resource efficiency and waste valorization. The optimized lithium leaching process achieved an efficiency of 95.0% (±2.3%). Additionally, tartaric acid recovery demonstrated a high yield of 98.0% (±1.9), allowing for its reuse in subsequent leaching cycles. Lithium precipitation as lithium phosphate resulted in a recovery yield of 97.7% (±3.6%),

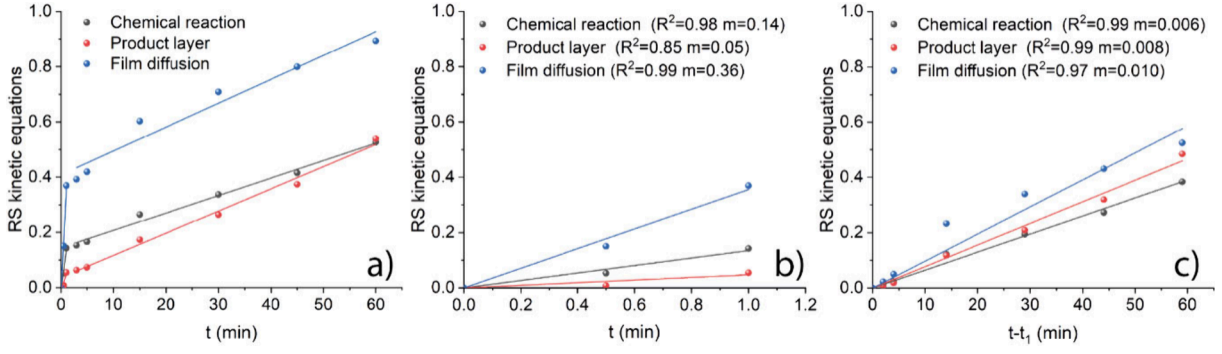


**Figure 4.** Right side (RS) of rate-controlling equations as a function of time at optimum conditions; (a) eqs 12–14, (b) eqs 12–14 (step 1), (c) eqs 15–17 (step 2).



https://doi.org/10.1021/acssusresmgt.4c00499
ACS Sustainable Resour. Manage. 2025, 2, 605–612

further confirming the efficiency of the method. The SCM demonstrated a good fit with the experimental data, allowing for determination of the rate constant for the leaching process. It was possible to accurately describe the kinetics of the process and extract meaningful information about the rate at which the desired reaction occurs. Overall, the optimized process offers a scalable and viable solution for lithium recovery, enhancing resource utilization and minimizing waste, thus contributing to the development of sustainable industrial practices. The application of experimental design techniques, such as factorial and central composite designs, was crucial in efficiently identifying and optimizing key process parameters, significantly improving the process's overall performance.

## ■ ASSOCIATED CONTENT

### Supporting Information

The Supporting Information is available free of charge at https://pubs.acs.org/doi/10.1021/acssusresmgt.4c00499.

Description of the ICP-OES, XRD, and SEM conditions, the experimental matrix and analysis plot of the DoE (both coded and uncoded), the diffraction pattern, and the FT-IR spectrum (PDF)

## ■ AUTHOR INFORMATION


### Corresponding Author

**Mario Berrettoni** − *School of Science and Technology, University of Camerino - ChIP Building, Camerino 62032, Italy;* orcid.org/0000-0002-2273-035X; Email: mario.berrettoni@unicam.it

### Authors

**Raffaele Emanuele Russo** − *School of Science and Technology, University of Camerino - ChIP Building, Camerino 62032, Italy*

**Alessio Giampaoli** − *School of Science and Technology, University of Camerino - ChIP Building, Camerino 62032, Italy*

**Martina Fattobene** − *School of Science and Technology, University of Camerino - ChIP Building, Camerino 62032, Italy*

**Paolo Cognigni** − *School of Science and Technology, University of Camerino - ChIP Building, Camerino 62032, Italy*

**Silvia Zamponi** − *School of Science and Technology, University of Camerino - ChIP Building, Camerino 62032, Italy*

**Paolo Conti** − *School of Science and Technology, University of Camerino - ChIP Building, Camerino 62032, Italy;* orcid.org/0000-0002-5469-5173

**Gabriele Giuli** − *School of Science and Technology, University of Camerino - Geology Division, Camerino 62032, Italy*

Complete contact information is available at: https://pubs.acs.org/10.1021/acssusresmgt.4c00499


### Notes

The authors declare no competing financial interest.

## ■ ACKNOWLEDGMENTS

We sincerely thank Engr. Alfredo Mancini, Engr. Roberta Vecchiola, and the entire research group of Orim S.p.a. for providing us with $LiFePO_4$ and Distillerie Mazzari S.p. for the tartaric acid recovered from winery industry wastes. The PhD grant of R.E.R. has been financed by PON funds from MIUR (CUP: J19J21018790001). The project benefited from MITE funds to G.G. and M.B. ('Ministero dell'Ambiente e della Tutela del Territorio e del Mare − Direzione Generale per l'Economia Circolare', 'Recupero di materiali critici da rifiuti elettronici', CUP: J13C22000320001) and UNICAM FAR funds to G.G. ('Recovery of critical metals (Pd, Ni, V, Cu, Ag, Sn, Au) from industrial waste (REMINE)', CUP: J15F22000020001).

## ■ REFERENCES


(1) Muchuweni, E.; Mombeshora, E. T.; Muiva, C. M.; Sathiaraj, T. S. Lithium-Ion Batteries: Recent Progress in Improving the Cycling and Rate Performances of Transition Metal Oxide Anodes by Incorporating Graphene-Based Materials. *Journal of Energy Storage* **2023**, *73*, 109013.

(2) Li, L.; Lu, J.; Zhai, L.; Zhang, X.; Curtiss, L.; Jin, Y.; Wu, F.; Chen, R.; Amine, K. A Facile Recovery Process of Cathodes from Spent Lithium Iron Phosphate Batteries by Using Oxalic Acid. *Journal of power and energy systems* **2018**, *4* (4), 219−225.

(3) Li, H.; Xing, S.; Liu, Y.; Li, F.; Guo, H.; Kuang, G. Recovery of Lithium, Iron, and Phosphorus from Spent LiFePO4 Batteries Using Stoichiometric Sulfuric Acid Leaching System. *ACS Sustain Chem. Eng.* **2017**, *5* (9), 8017−8024.

(4) Mahandra, H.; Ghahreman, A. A Sustainable Process for Selective Recovery of Lithium as Lithium Phosphate from Spent LiFePO4 Batteries. *Resour Conserv Recycl* **2021**, *175*, 105883.

(5) Kumar, J.; Shen, X.; Li, B.; Liu, H.; Zhao, J. Selective Recovery of Li and FePO4 from Spent LiFePO4 Cathode Scraps by Organic Acids and the Properties of the Regenerated LiFePO4. *Waste Management* **2020**, *113*, 32−40.

(6) Rautela, R.; Yadav, B. R.; Kumar, S. A Review on Technologies for Recovery of Metals from Waste Lithium-Ion Batteries. *J. Power Sources* **2023**, *580*, 233428.

(7) Liu, A.; Hu, G.; Wu, Y.; Guo, F. Life Cycle Environmental Impacts of Pyrometallurgical and Hydrometallurgical Recovery Processes for Spent Lithium-Ion Batteries: Present and Future Perspectives. *Clean Technol. Environ. Policy* **2024**, *26* (2), 381−400.

(8) Golmohammadzadeh, R.; Faraji, F.; Rashchi, F. Recovery of Lithium and Cobalt from Spent Lithium Ion Batteries (LIBs) Using Organic Acids as Leaching Reagents: A Review. *Resources, Conservation and Recycling* **2018**, *136*, 418−435.

(9) Xiao, X.; Hoogendoorn, B. W.; Ma, Y.; Ashoka Sahadevan, S.; Gardner, J. M.; Forsberg, K.; Olsson, R. T. Ultrasound-Assisted Extraction of Metals from Lithium-Ion Batteries Using Natural Organic Acids. *Green Chem.* **2021**, *23* (21), 8519−8532.

(10) He, L. P.; Sun, S. Y.; Mu, Y. Y.; Song, X. F.; Yu, J. G. Recovery of Lithium, Nickel, Cobalt, and Manganese from Spent Lithium-Ion Batteries Using l -Tartaric Acid as a Leachant. *ACS Sustain Chem. Eng.* **2017**, *5* (1), 714−721.

(11) Kontogiannopoulos, K. N.; Patsios, S. I.; Karabelas, A. J. Tartaric Acid Recovery from Winery Lees Using Cation Exchange Resin: Optimization by Response Surface Methodology. *Sep Purif Technol.* **2016**, *165*, 32−41.

(12) Devesa-Rey, R.; Vecino, X.; Varela-Alende, J. L.; Barral, M. T.; Cruz, J. M.; Moldes, A. B. Valorization of Winery Waste vs. the Costs of Not Recycling. *Waste Management* **2011**, *31* (11), 2327−2335.

(13) Leardi, R.; Melzi, C.; Polotti, G. *CAT (Chemometric Agile Tool)*.

(14) Ebrahimi-Najafabadi, H.; Leardi, R.; Jalali-Heravi, M. Experimental Design in Analytical Chemistry -Part I: Theory. *Journal of AOAC International* **2014**, *97*, 3−11.

(15) Leardi, R. Experimental Design in Chemistry: A Tutorial. *Anal Chim Acta* **2009**, *652* (1-2), 161−172.

(16) Li, L.; Fan, E.; Guan, Y.; Zhang, X.; Xue, Q.; Wei, L.; Wu, F.; Chen, R. Sustainable Recovery of Cathode Materials from Spent Lithium-Ion Batteries Using Lactic Acid Leaching System. *ACS Sustain Chem. Eng.* **2017**, *5* (6), 5224−5233.

(17) Shin, D. J.; Joo, S. H.; Lee, D.; Shin, S. M. Precipitation of Lithium Phosphate from Lithium Solution by Using Sodium

Phosphate. *Canadian Journal of Chemical Engineering* **2022**, *100* (12), 3760−3767.
(18) Annunzi, F.; Nicolella, C.; Stella, R. S.; Lenzi, M.; Signorini, F. Recovery of Lithium from Brine by Phosphate Precipitation. *Chem. Eng. Trans* **2023**, *98*, 207−212.
(19) Xiao, C.; Zeng, L. Thermodynamic Study on Recovery of Lithium Using Phosphate Precipitation Method. *Hydrometallurgy* **2018**, *178*, 283−286.
(20) Li, H.; Xing, S.; Liu, Y.; Li, F.; Guo, H.; Kuang, G. Recovery of Lithium, Iron, and Phosphorus from Spent LiFePO4 Batteries Using Stoichiometric Sulfuric Acid Leaching System. *ACS Sustain Chem. Eng.* **2017**, *5* (9), 8017−8024.
(21) Yang, Y.; Meng, X.; Cao, H.; Lin, X.; Liu, C.; Sun, Y.; Zhang, Y.; Sun, Z. Selective Recovery of Lithium from Spent Lithium Iron Phosphate Batteries: A Sustainable Process. *Green Chem.* **2018**, *20* (13), 3121−3133.
(22) Levenspiel, O. *Chemical Reaction Engineering*; Wiley, 1998.
(23) Habbache, N.; Alane, N.; Djerad, S.; Tifouti, L. Leaching of Copper Oxide with Different Acid Solutions. *Chem. Eng. J.* **2009**, *152* (2-3), 503−508.
(24) Moretti, A.; Giuli, G.; Nobili, F.; Trapananti, A.; Aquilanti, G.; Tossici, R.; Marassi, R. Structural and Electrochemical Characterization of Vanadium-Doped LiFePO 4 Cathodes for Lithium-Ion Batteries. *J. Electrochem Soc.* **2013**, *160* (6), A940−A949.
(25) https://chemaxon.com.
(26) Chen, X.; Kang, D.; Cao, L.; Li, J.; Zhou, T.; Ma, H. Separation and Recovery of Valuable Metals from Spent Lithium Ion Batteries: Simultaneous Recovery of Li and Co in a Single Step. *Sep Purif Technol.* **2019**, *210*, 690−697.
(27) Musariri, B.; Akdogan, G.; Dorfling, C.; Bradshaw, S. Evaluating Organic Acids as Alternative Leaching Reagents for Metal Recovery from Lithium Ion Batteries. *Miner Eng.* **2019**, *137*, 108−117.
(28) Kostromina, N. A.; Trunova, E. K.; Tananaeva, N. N. Complex Formation of Fe(III) with Tartaric Acid by the Method of Nuclear Magnetic Relaxation. *Theor. Exp. Chem.* **1988**, *23*, 462−466.
(29) Yokoi, H.; Mitani, T.; Mori, Y.; Kawata, S. Complex Formation between Iron (III) and Tartaric and Citric Acids in a Wide PH Range 1 to 13 as Studied by Magnetic Susceptibility Measurements. *Chem. Lett.* **1994**, *23* (2), 281−284.
(30) European Commission. https://eur-lex.europa.eu/legal-content/EN/ALL/?uri=CELEX%3A32012R0231.
(31) Lide, D. R. Solubility Product Constants. In *CRC Handbook of Chemistry and Physics*, 87th ed.; 2007.
(32) Vyas, P.; Jethva, H.; John Joshi, S.; Janakrai Joshi, M. Roles of Gel Medium and Gelling Solution in the Growth of the Crystals: A Case Study of Calcium Levo-Tartrate. *Arch. Phy. Res.* **2013**, *4* (6), 9−15.
(33) Shajan, X. S.; Mahadevan, C. On the Growth of Calcium Tartrate Tetrahydrate Single Crystals. *Bull. Mater. Sci.* **2004**, *27*, 327−331.
(34) Kontogiannopoulos, K. N.; Patsios, S. I.; Karabelas, A. J. Tartaric Acid Recovery from Winery Lees Using Cation Exchange Resin: Optimization by Response Surface Methodology. *Sep Purif Technol.* **2016**, *165*, 32−41.
(35) Zhang, K.; Wang, M.; Wang, D.; Gao, C. The Energy-Saving Production of Tartaric Acid Using Ion Exchange Resin-Filling Bipolar Membrane Electrodialysis. *J. Memb Sci.* **2009**, *341* (1-2), 246−251.
(36) Traving, M.; Bart, H.-J. Recovery of Organic Acids Using Ion-Exchanger-Impregnated Resins. *Chem. Eng. Technol.* **2002**, *25* (10), 997−1003.
(37) Andres, L. J.; Riera, F. A.; Alvarez, R. Recovery and Concentration by Electrodialysis of Tartaric Acid from Fruit Juice Industries Waste Waters. *J. Chem. Technol. Biotechnol.* **1997**, *70*, 247.
(38) Kaya, C.; Şahbaz, A.; Arar, Ö.; Yüksel, Ü.; Yüksel, M. Removal of Tartaric Acid by Gel and Macroporous Ion-Exchange Resins. *Desalination Water Treat* **2015**, *55* (2), 514−521.
(39) Ben Bechir, M.; Ben Rhaiem, A. The Lithium-Ion Battery: Study of Alternative Current Conduction Mechanisms on the Li3PO4 - Based Solid Electrolyte. *Physica E Low Dimens Syst. Nanostruct* **2021**, *130*, 114686.
(40) Benoy, S. M.; Singh, S.; Pandey, M.; Manoj, B. Characterization of Nanocarbon Based Electrode Material Derived from Anthracite Coal. *Mater. Res. Express* **2019**, *6* (12), 125624.
(41) Wongnaree, N.; Yingnakorn, T.; Ma-Ud, N.; Sriklang, L.; Khumkoa, S. Recovery of Valuable Metals from Leached Solutions of Black Mass through Precipitation Method. *Results in Engineering* **2025**, *25*, 104190.
(42) Aarabi-Karasgani, M.; Rashchi, F.; Mostoufi, N.; Vahidi, E. Leaching of Vanadium from LD Converter Slag Using Sulfuric Acid. *Hydrometallurgy* **2010**, *102* (1-4), 14−21.